PSEUDO-REALISTIC GEANT4 SIMULATION OF A 44/88 MHZ COOLING CHANNEL FOR THE NEUTRINO FACTORY

V.D. Elvira[1], H. Li[2], P. Spentzouris[1]
[1]Fermilab, Batavia, IL 60510, USA
[2]ITT, Chicago, IL, USA

Abstract

A muon cooling channel design for a neutrino factory, based on low frequency 44/88 MHz r.f. technology, has been recently developed at CERN [1]. This scheme is an interesting alternative to the options developed in the US, based on 201 MHz r.f. systems [2], as well as a candidate for the International Muon Cooling Exeriment. We designed and simulated a pseudo-realistic version of the three sections of the CERN cooling channel. We verified that the GEANT4 and PATH simulations of the hard-edge version of the 44 MHz section give consistent results. We studied the performance of the pseudo-realistic 44 MHz section and suggested modifications/improvements to the current design.

1 INTRODUCTION

A muon cooling channel design for a neutrino factory, based on low frequency 44/88 MHz r.f. technology, has been recently developed at CERN [1]. This scheme is an interesting alternative to the options developed in the US, based on 201 MHz r.f. systems [2]. The main difference between the low frequency and the high frequency designs is that the former scheme makes use of the pion beam micro-structure to avoid re-bunching before cooling. In the latter design, on the other hand, the cooling channel is preceeded by a bunching section. The larger bucket associated with the lower frequency design helps to reduce longitudinal losses in the cooling section, although at the expense of a substantial longitudinal emittance growth.

A descrition as well as a simulation of the low frequency system is available in Ref. [1].The simulation is based on the PATH program [3], used in fast mode, within the paraxial approximation. Hard edge magnetic fields, and infinitely thin cavities are implemented.

In this note, we used the GEANT4 [4] tool kit to perform a pseudo-realistic simulation of the 44/88 MHz cooling channel. GEANT4 is a tracking code which performs a full integration of the equation of motion.

The objective of our study was to investigate the transition from a simple to a realistic simulation of the 44/88 MHz channel, using realistic fields associated with r.f. cavities and solenoids. The simulation is “pseudo”-realistic in the sense that cavity or absorber windows and engineering constraints are not fully studied and incorporated. The simulation code was implemented for the three sections of the channel (first cooling, acceleration, second cooling). It is flexible to allow changes in the lattice, r.f., absorber, and beam parameters, whenever the design is stable and ready for optimization. Modifications will be needed as the cooling channel is integrated to a more detailed

design of the front-end and succeeding accelerator sections.

There is an on-going effort[5] to replace the 44 MHz r.f. system in the first cooling section and make it 88 MHz all through the channel. We therefore did not attempt to optimize the current lattice or beam parameters at this stage.

2 GENERAL DESCRIPTION OF THE NEUTRINO SOURCE DESIGN

A pion beam is generated from a 2.2 GeV proton beam interacting with a mercury target inmersed in a 20 T solenoid. The pions decay in a 30 m long channel inside a 1.8 Tesla solenoid. At the end of this decay channel, the particles with kinetic energy in the range 100-300 MeV enter a phase rotation section, which uses 44 MHz cavities to reduce the energy spread by about a factor of two. The first cooling stage uses the same lattice and r.f. system as the phase rotation section but includes liquid hydrogen absorbers to reduce the transverse emittance by a factor of about 0.7 in each plane. The lattice is further extended, without absorbers in an acceleration section which increases the beam average energy from 200 MeV to about 280 MeV. At this point, the beam size is small enough to allow a second cooling section, based on 88 MHz cavities, to reduce the transverse emittance by approximately a factor of four in each plane. After cooling, the beam energy is ramped up to 2 GeV, suitable for injection in a μRLA, using two accelerator sections with cavities operated at 88 MHz and 176 MHz, respectively.

The general design as well as the specific values of the parameters of the channels described in the following sections followed, when available, the information in Ref. [1, 5].

3 THE COOLING CHANNEL

The first step in our study was to compare PATH simulation results [1] with those obtained using GEANT4. We therefore wrote simulation code for the 44 MHz cooling section following exactly the CERN hard-edge design.

A realistic version of the hard-edge cooling channel was not available. The second step, and primary goal of this study, was to design a realistic channel which followed as closely as possible the hard-edge design. Realistic r.f. and solenoidal fields were extracted from Ref. [6, 7].

3.1 Hard-Edge Version of the 44 MHz Section

A representation of a unit cell of the hard-edge 44 MHz section is shown in Fig. 1. It is composed of two sub-cells, 2 m long each, with ideal solenois producing a square B_z field of 2 T constant in the radial direction. This periodic square field alternates between $+2$ T and -2 T, and takes zero value at 5 mm before and after every transition, where B_r is non-zero. The radial field is zero except in this region of transition where, following from the integration of Maxwell equations:

$$\frac{1}{r}\frac{\partial}{\partial r}\left(rB_r\right) = -\frac{\partial B_z}{\partial z}$$

$$B_r = -(r/2) \times \left(\Delta B_z/\Delta z\right),$$

with $\Delta B_z = \pm 4$ T and Δz=1 cm. The azimuthal and radial components of the magnetic field are shown in Figs. 2 and 3. They are input to GEANT4 in the form of field maps.

The hard-edge channel is a resonance free system. This follows from the equation of betatron oscillations. In the Larmor frame, under the paraxial approximation, it becomes:

$$\frac{d^2x}{dz^2} + \left(\frac{eB_z(z)}{2pc}\right)^2 x = 0 \tag{1}$$

where x is any transverse coordinate, and p the particle momentum. The longitudinal field on axis $B_z(z) = B_\circ$ and, therefore, the β-function is a constant. Our implementation of a hard-edge channel, however, is not a completely resonance free system due to the contribution of the small zero field ranges in the field flip regions.

At 50 cm from the beginning of the cell, and then every 1 m, r.f. acceleration is achieved through a 2 MeV kick over a 1 cm region. A liquid Hydrogen (LH2) absorber, 27.7 cm long and 30 cm in radius, is located at the end of the cell. The r.f. system (vertical bars), and the absorber (grey block) are shown in Fig. 1. The length of the unit cell is 4.32 m, and the total length of the 44 MHz section, for 11 cells, 47.52 m

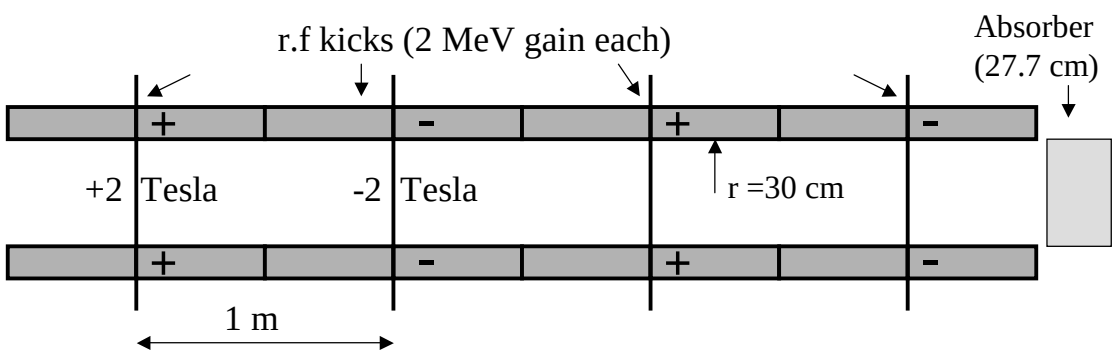

Figure 1: Representation of a unit cell of the hard-edge version of the 44 MHz cooling section. The dark grey blocks represent the solenoids, the vertical lines show the location of the r.f. kicks, and the light grey rectangle the LH2 absorber.

The r.f. is run on crest, to use the cavities at full power [5]. The synchronous phase of the cavities was therefore set to 90°. The r.f. system was tuned for a channel with nominal kinetic energy of 200 MeV, through the whole length of the channel. A nominal particle with that energy, at $x = y = 0$ and with zero transverse momentum, receives 8 MeV from the r.f. system and losses 8 MeV at the absorber. Fig. 4 shows the kinetic energy of the nominal particle as a function of the channel length z. In each cell, the four sections of almost instantaneous acceleration are followed by four associated drift regions. At the end of each cell, the particle loses the previously gained energy.

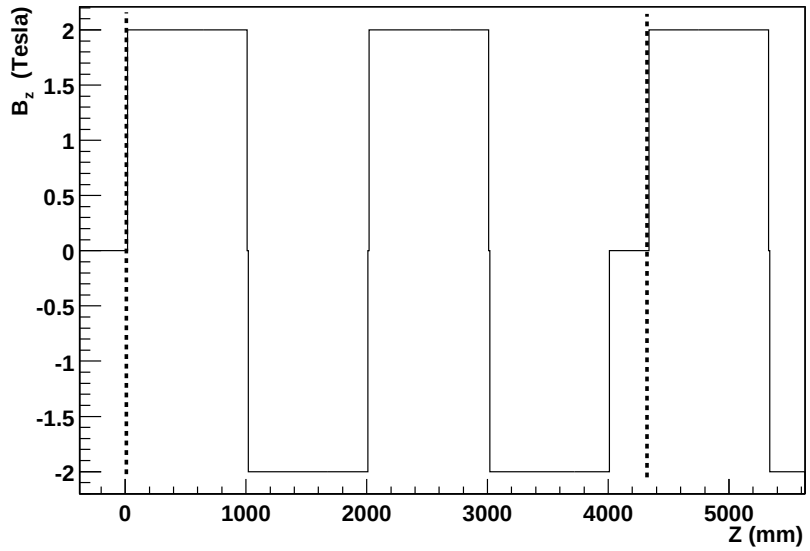

Figure 2: B_z versus z. Note the zero field regions at the transition points.

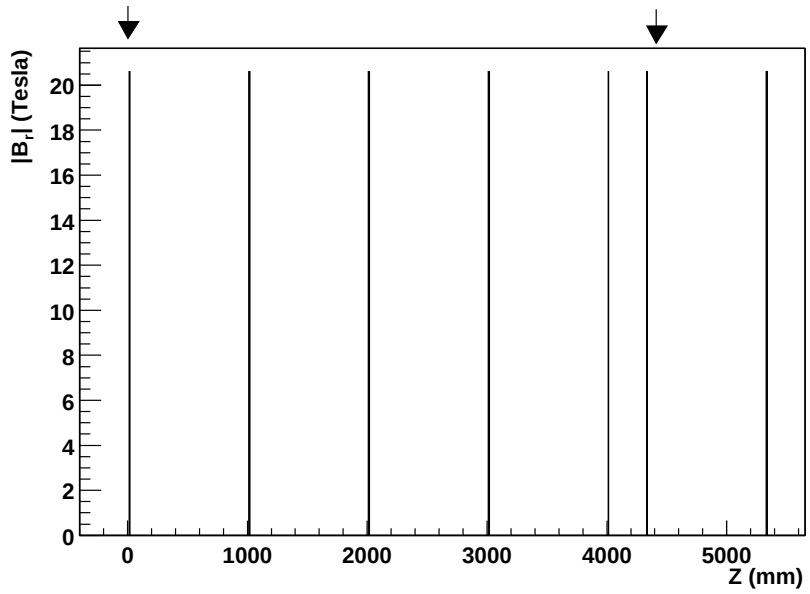

Figure 3: $|B_r|$ versus z at r=10.3 cm.The spikes are 0.5 cm long at z=0, $\approx$4 m, and $\approx$4.32 m, where B_z changes by $\pm$2 T. The spikes are 1 cm in the other locations, where B_z changes by $\pm$4 T. The arrows show the physical limits of a unit cell.

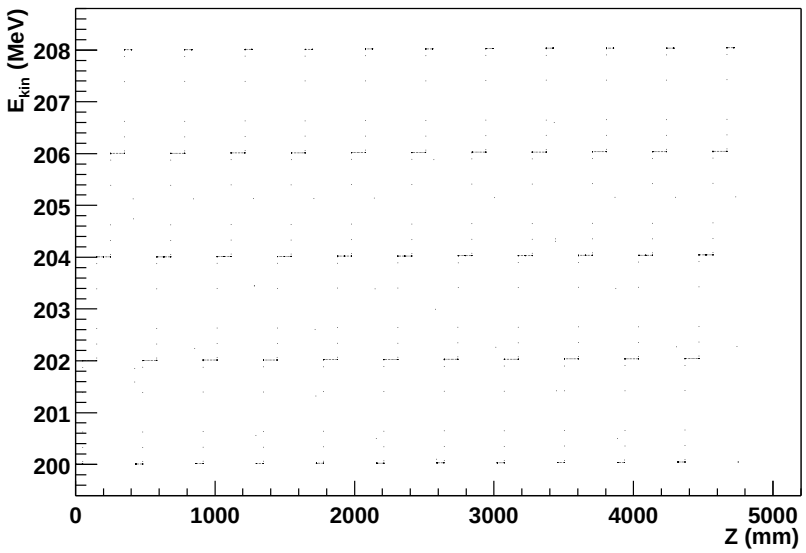

Figure 4: Kinetic energy of the nominal particle versus z, along the 11 cells of the 44 MHz cooling section.

3.2 *Pseudo-realistic Design*

We designed a pseudo-realistic cooling channel which follows the hard-edge lattice as closely as possible and is consistent with the cavity design in Ref. [6]. The channel consists of three parts. The first and second sections are 11 and 7 unit cells long, use the same lattice with 44 MHz cavities. The third section is 10 cells long, has the same lattice structure but different dimensions, and uses 88 MHz cavities. Cooling is performed at a constant nominal energy in the first and third sections. The second section, which does not contain absorbers, accelerates the beam in between the two cooling sections.

Geometry A scheme of the 44 MHz (88 MHz) cavities assembled with solenoids is shown in Figs. 5- 6. The cavities are 1.4 m (0.9 m) long and 0.3 m (0.15 m) in radius. They surround the solenoids, 88 cm (40 cm) long and 20 cm thick.

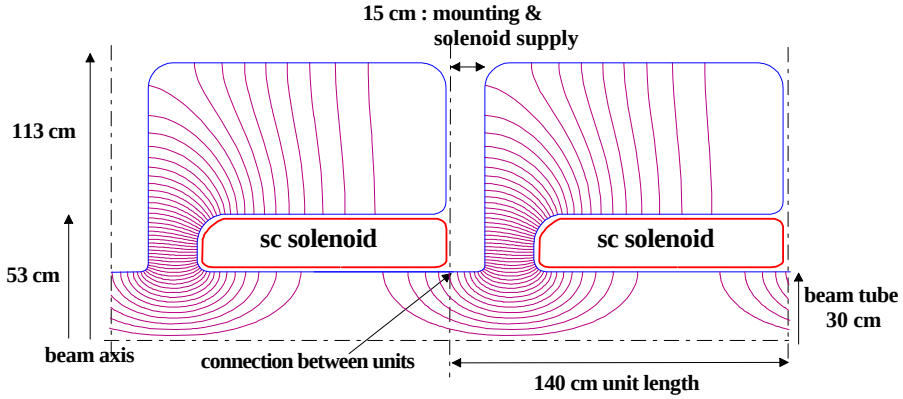

Figure 5: Scheme of the assembly of 44 MHz cavities with solenoids.

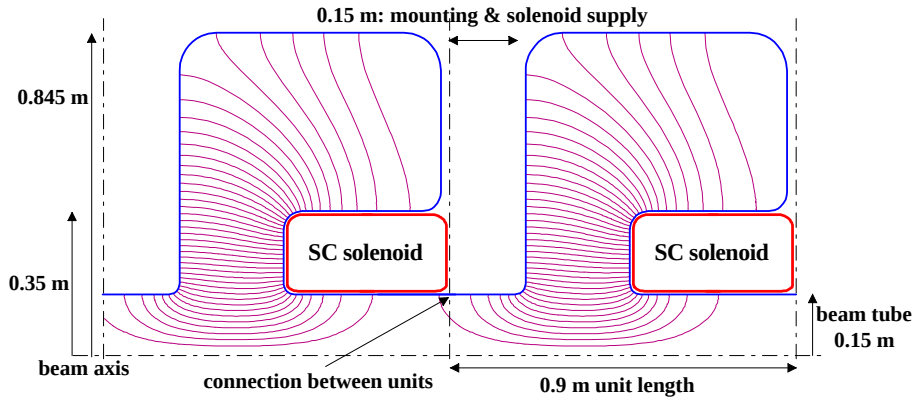

Figure 6: Scheme of the assembly of 88 MHz cavities with solenoids.

A unit cell is composed of four solenoids embedded in r.f. cavities as described in the previous paragraph, followed by a LH2 absorber 37 cm (51 cm) long in the case of the 44 MHz (88 MHz) section. Figure 7 shows a scheme of a 44 MHz (88 MHz) cooling cell, which is 6.04 m (4.24 m) long. The drawing shows the limits of the r.f. field maps used in the simulation, which does not extend beyond the inner radius of the solenoids. The length and radius of the cavities impose large gaps between magnets, 52 cm (40 cm) long. Note that the lattice has double periodicity due to the extra space needed to fit the absorber, shown as a light grey rectangle immediately before the end of the unit cell. The absorbers are longer than those in the hard-edge design to account for the higher gradient associated with the realistic cavities. Other equally valid choices consistent with the hard-edge design are a shorter absorber with only three r.f. cavities, or a shorter absorber with four cavities ran at a lower gradient.

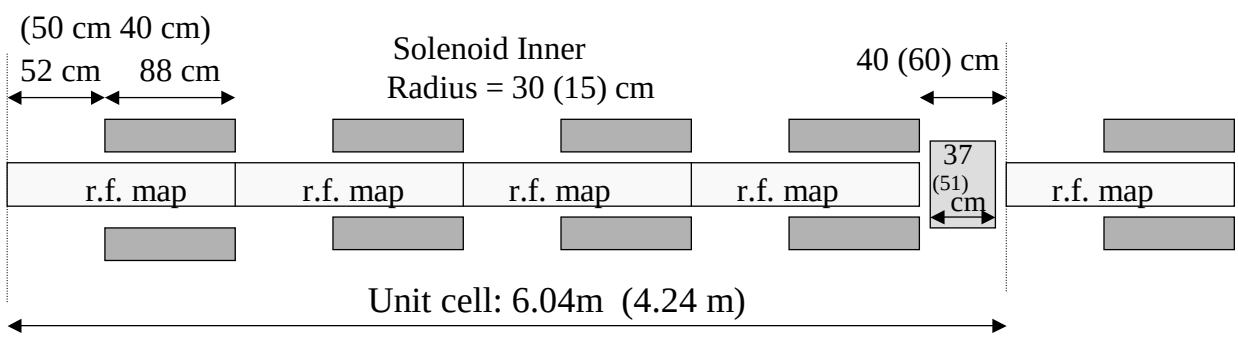

Figure 7: Scheme of 44 MHz (88 MHz) cooling cell. The dashed lines show the limits of the unit cell. The dark grey blocks represent the solenoids and the light grey rectangle the LH2 absorber.

Figure 8 shows a visualization of the geometry implemented in GEANT4. A view of the channel is shown on the left, and the detail of a unit cell on the right. The blue rings are the solenoid coils, and the red cylinders a representation of the r.f. field maps. The absorbers are the smaller short cylinders in grey.

Magnets The magnetic fields are not read out from field maps but generated analytically from electric currents through the solenoids. The current through the solenoids in the 44 MHz section is 12 A/mm^2, the value which maximizes transmission. The two components of the solenoidal field,

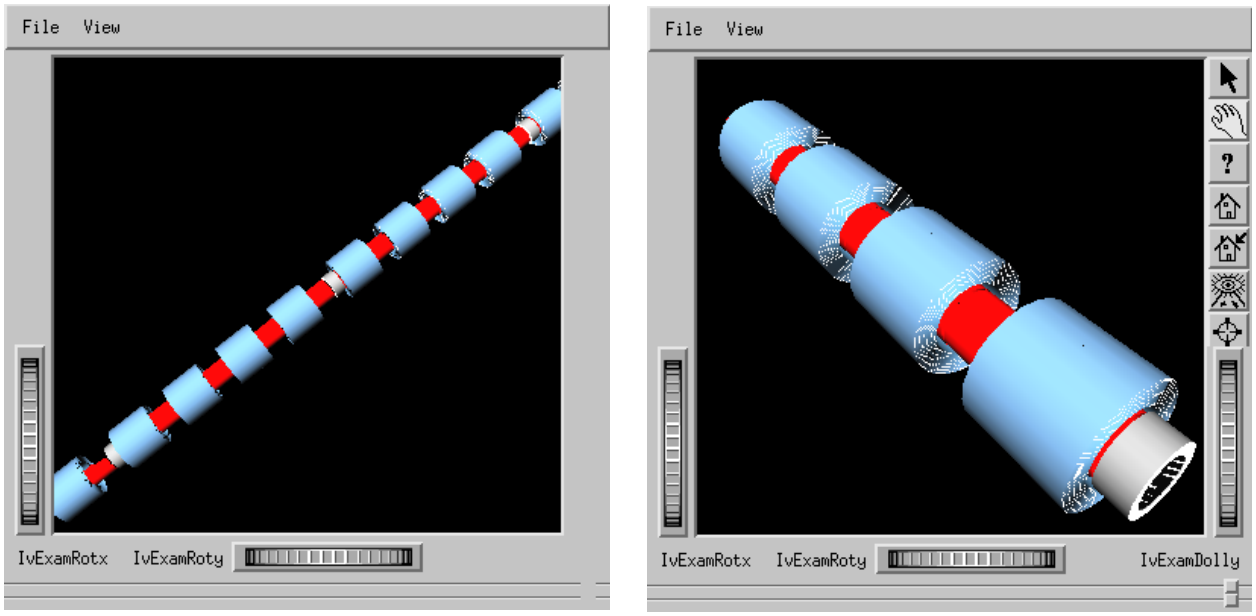

Figure 8: Left: visualization of the channel geometry as implemented in GEANT4. Right: detail of a unit cell. The blue rings are the solenoid coils, and the red cylinders a representation of the r.f. field maps. The absorbers are the smaller short cylinders in grey.

B_z and B_r, are quite different in the pseudo-realistic and the hard-edge cells. Fig. 3.2 shows B_z on axis as a function of z in a unit cell, delimited by the vertical lines. The absorber is located immediately before the dashed line on the right. The field is closer to a sine than to a square function, unlike the hard-edge case which is a perfect square. Note the double periodicity of the lattice, which manifests as a modulation (shoulder) every two periods of the dominant frequency. The absorber is not located in a zero field region as in the hard-edge version. Fig. 9 shows $|B_r|$ as a function of z at r=10.3 cm. Again, it looks quite different from the ideal hard-edge case. The radial field is not delta-like but extends over all space. The peaks are double, due to the gaps between solenoids, and their amplitude changes in the absorber region due to the extra gap. Figures 10 shows the magnetic fields for an 88 MHz cooling cell. The currents were not optimized for maximum transmission. Note that the modulation to the field is larger than in the 44 MHz cell.

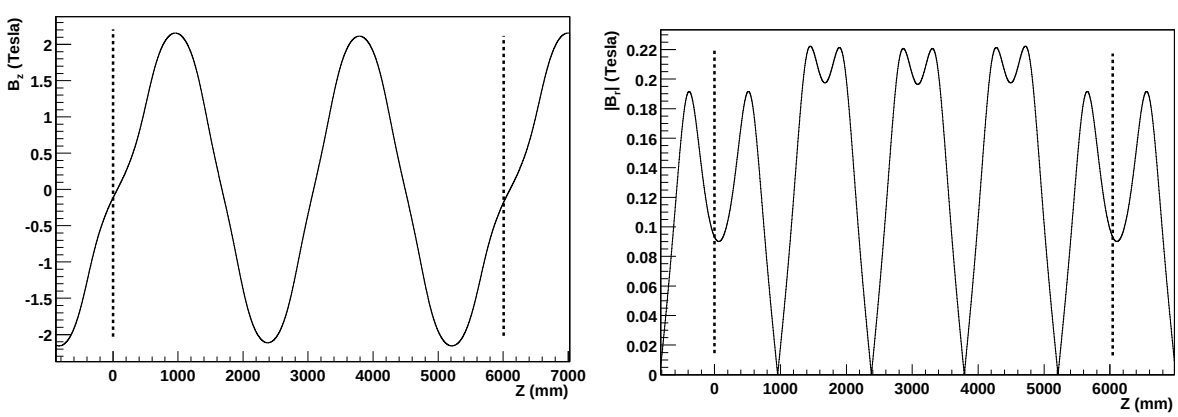

Figure 9: Left: $|B_z|$ versus z at r=10.3 cm for the 44 MHz cooling cell. The dashed bars show the limits of cell. Right: $|B_r|$ versus z on axis.

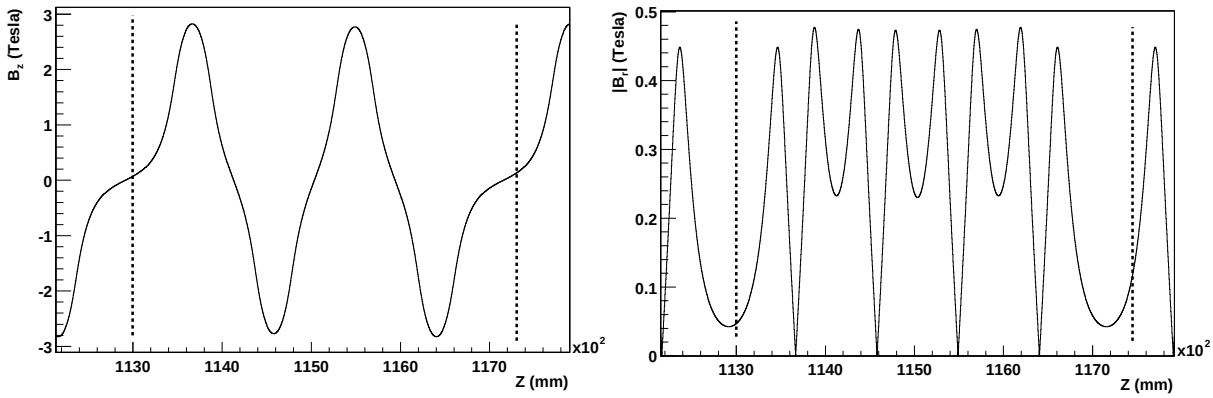

Figure 10: Left: B_z versus z on axis for the 88 MHz cooling cell. The dashed bars show the limits of cell. Right: $|B_r|$ versus z at r=10.3 cm.

In the case of a sinusoidal longitudinal field on axis, somewhat close to the case we are studying, Eq. 1 reduces to:

$$\frac{d^2x}{dz^2} + x\left(\frac{eB_\circ}{2pc}\right)^2 \sin\frac{\pi z}{L} = 0 \tag{2}$$

where $2L$ is the period length [8]. The 2π and π resonances are located at:

$$\frac{2pc}{eB_\circ L} = [0.09, 0.12] \text{ and } [0.17, 0.28]\,, \text{ respectively } . \tag{3}$$

Acceleration Realistic field maps associated with the cavities in Figs. 5- 6 were provided by CERN [7] and incorporated in the GEANT4 simulation. Cavity specifications are available in Ref. [6]. If ran on crest, each 44 MHz (88 MHz) cavity would provide a gradient of approximately 2 MeV/m (4 MeV/m). More precisely:

$$\int\int z\, E_z(r=0)\, dz\, dt = 2.87 \text{ MeV in } 1.4 \text{ m } (44 \text{ MHz})$$

$$\int\int z\, E_z(r=0)\, dz\, dt = 3.73 \text{ MeV in } 0.9 \text{ m } (88 \text{ MHz})$$

The transit time factor reduces the effective gradient to ≈ 1.95 MeV (3.95 MeV), respectively. The four cavities in each cell restore the ≈ 10.9 MeV (14.2 MeV) lost by a nominal particle with E_{kin}=200 MeV. The r.f. system was run on crest, at a synchronous phase of 90° [5]. The phases were set at the E_z (z component of the electric field) weighted z (longitudinal position) mean along the cavity: 27.3 cm (16.3 cm). The r.f. tuning is shown in Fig 11. A particle, with initial E_{kin} =200 MeV and $x = y = p_x = p_y = 0$, is run through the channel to adjust the cavity phases so that the particle follows a pre-defined channel nominal energy. That nominal kinetic energy is 200 MeV in the first cooling section (44 MHz cavities), and 275 MeV in the second cooling section (88 MHz cavities). The energy is ramped-up from 200 MeV to 275 MeV in the intermediate (acceleration with no absorbers) section.

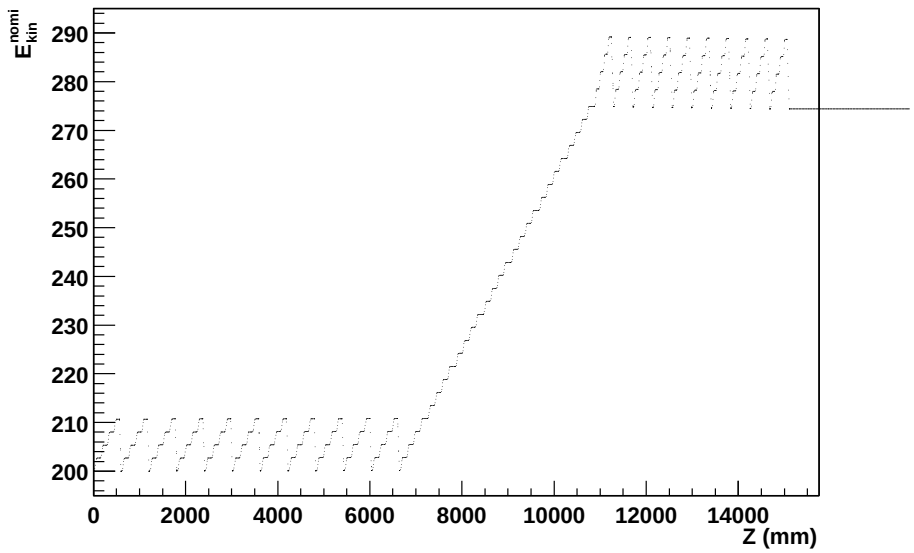

Figure 11: Nominal Kinetic energy of the channel as a function of z. The plot shows the actual trajectory, in E_{kin}-z space, of the "nominal" particle used to tune the synchronous phases of the r.f. cavities. Random processes, like multiple scattering and straggling, were turned off for the tuning.

3.3 The Beam

The 5100 particles input beam used in these studies was provided by CERN [5]. It is the output beam of the hard-edge simulation of the phase rotation section in Ref. [1], with a $|cT - cT_o| < 85$ cm cut in the bunch length. The actual beam is not as uniform in energy-cT space as shown in Fig. 13. The $|cT - cT_o| < 85$ cut removes the tails (see Fig.3 in Ref. [1]) from fast particles with energy greater than average and slow particles with energy lower than average. In our study, we derive transmission numbers relative to the initial beam rather than the absolute number of muons per proton.

The beam is injected at the origin ($z = 0$) of the 44 MHz section in both the hard-edge and pseudo-realistic simulations described in this note. Table 1 lists the initial beam parameters.

Table 1: Parameters of the beam injected at the origin of the cooling channel. The average kinetic energy is 200 MeV, $< x >=< y >=< p_x >=< p_y >= 0$.

σ_x	σ_{p_x}	$\sigma_x \sigma_{p_x}/mc$	σ_{cT}	σE	ε_x
(cm)	**(MeV/c)**	**(cm)**	**(cm)**	**(MeV)**	**(cm)**
10.9	29.4	3.03	48.1	13.9	2.51

Figures 12-13 show the initial beam distributions. The non-zero angular momentum manifests as a $p_y - x$ correlation, which should provide the matching to the hard-edge design of the first cooling section.

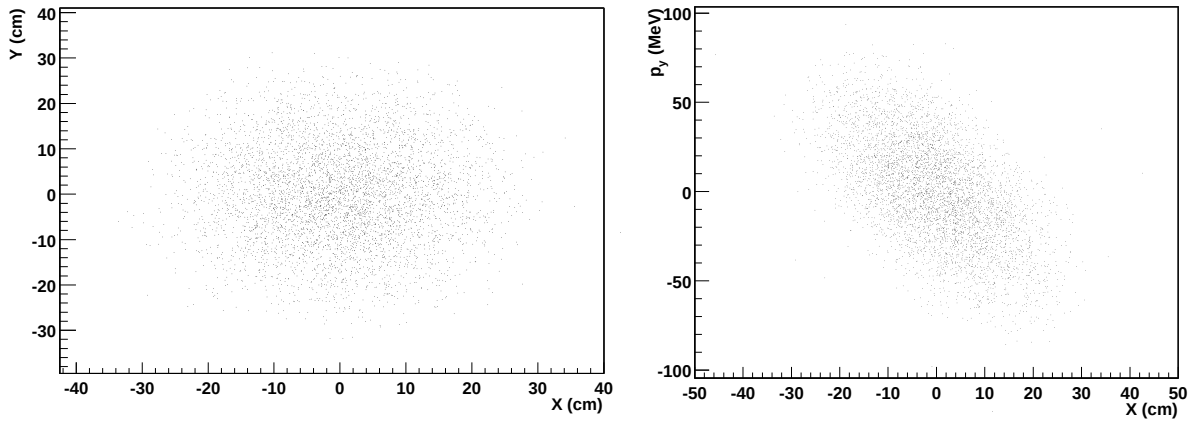

Figure 12: y versus x (left) and p_y versus x for the initial beam.

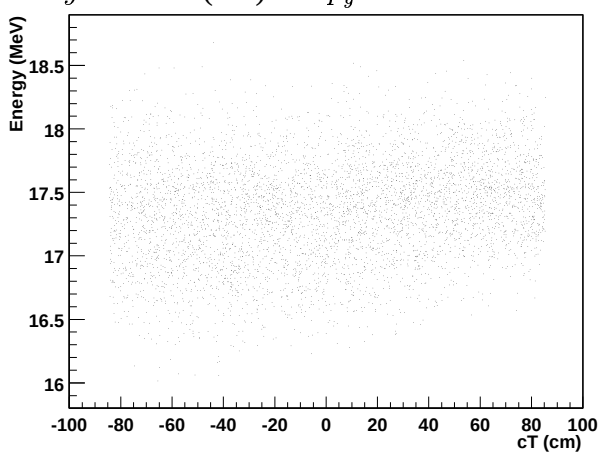

Figure 13: E versus cT for the initial beam.

4 PERFORMANCE

4.1 Hard-Edge Results

Only the 44 MHz section is studied because the goal was to compare our GEANT4 implementation with the PATH simulation in Ref. [1] Fig. 14 is based on a 5100 particles simulation and illustrates the performance of the 44 MHz section of the channel. Transverse emittance is defined (see Ref. [9]) as:

$$\varepsilon_T = \frac{\sqrt{\det|M|}}{(m_\mu c^2)^2} \,,$$

with M the second moments matrix in transverse phase space. The transverse emittance in each plane is defined as $\varepsilon_x = \sqrt{\varepsilon_T}$. Correlations are included in the calculations. While σ_{p_x} remains basically constant along the channel, σ_x diminishes from 10.9 cm to 8.7 cm. Transverse emittance decreases from 25.1 mm to 17 mm, yielding a 0.68 cooling factor in each transverse direction. Reference [1] reports a similar value for an equivalent system. Transmission is 86.3%, against the

97% reported in Ref. [1]. We observe initial losses which are probably due to beam mis-match, and the fact that the solenoid inner radius (30 cm) is less than 3 times σ_x of the initial beam ($\approx$ 33 cm). Transmission stabilizes to a fairly constant value but drops at the end of the section due to longitudinal losses.

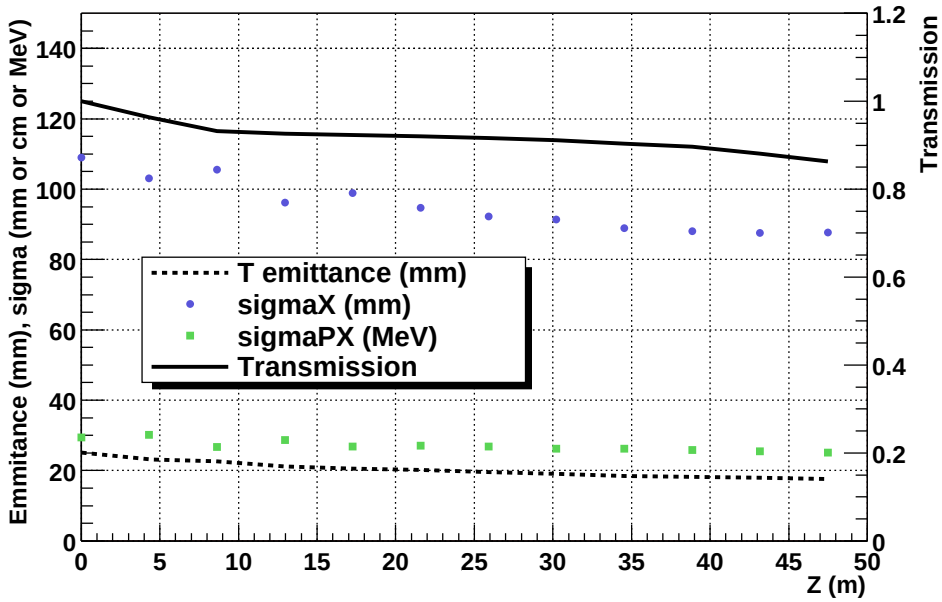

Figure 14: Performance of the hard-edge version of the 44 MHz section of the cooling channel. Transverse emittance stands for ε_x.

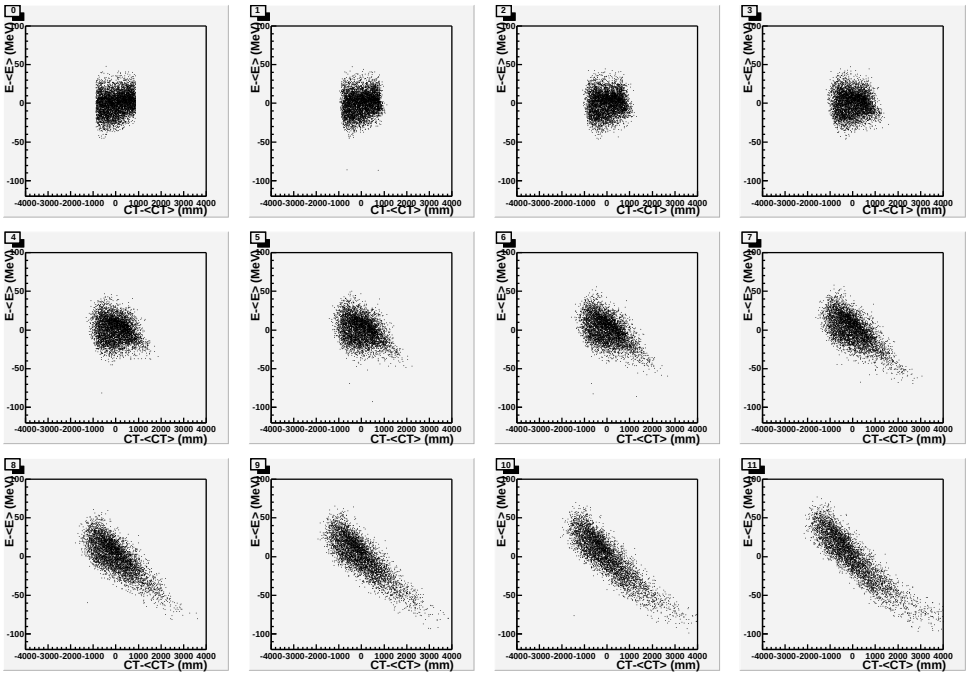

Figure 15: Evolution of longitudinal phase space along the hard edge 44 MHz section. Each plot is a snapshot of the beam at the end of each cooling cell.

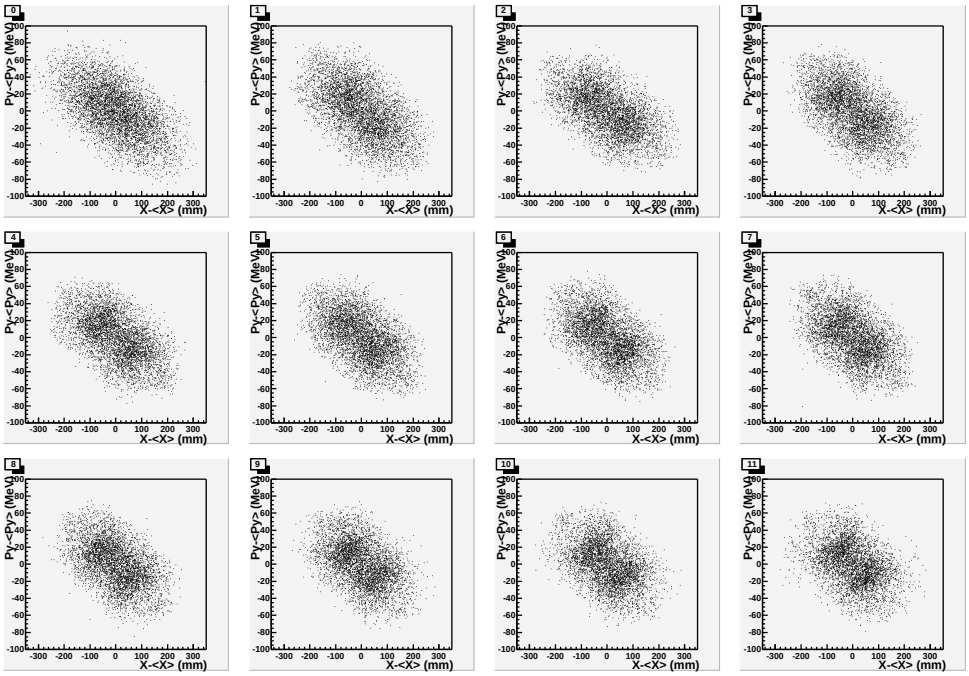

Figure 16: Evolution of the angular momentum along the hard edge 44 MHz section. Each plot is a snapshot of the beam at the end of each cooling cell.

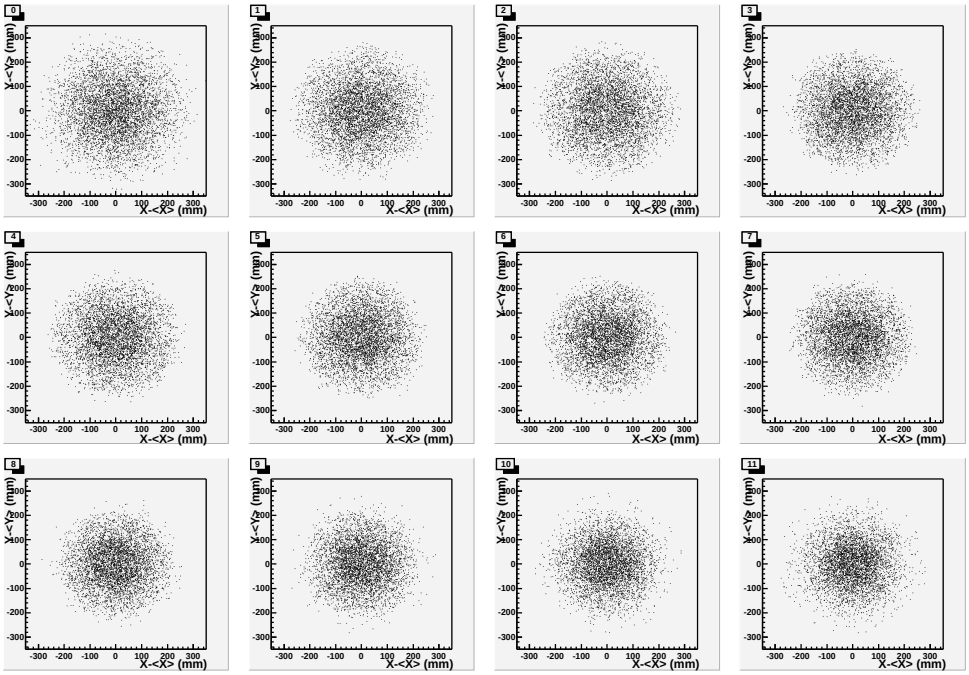

Figure 17: Evolution of the transverse physical size of the beam along the hard edge 44 MHz section. Each plot is a snapshot of the beam at the end of each cooling cell.

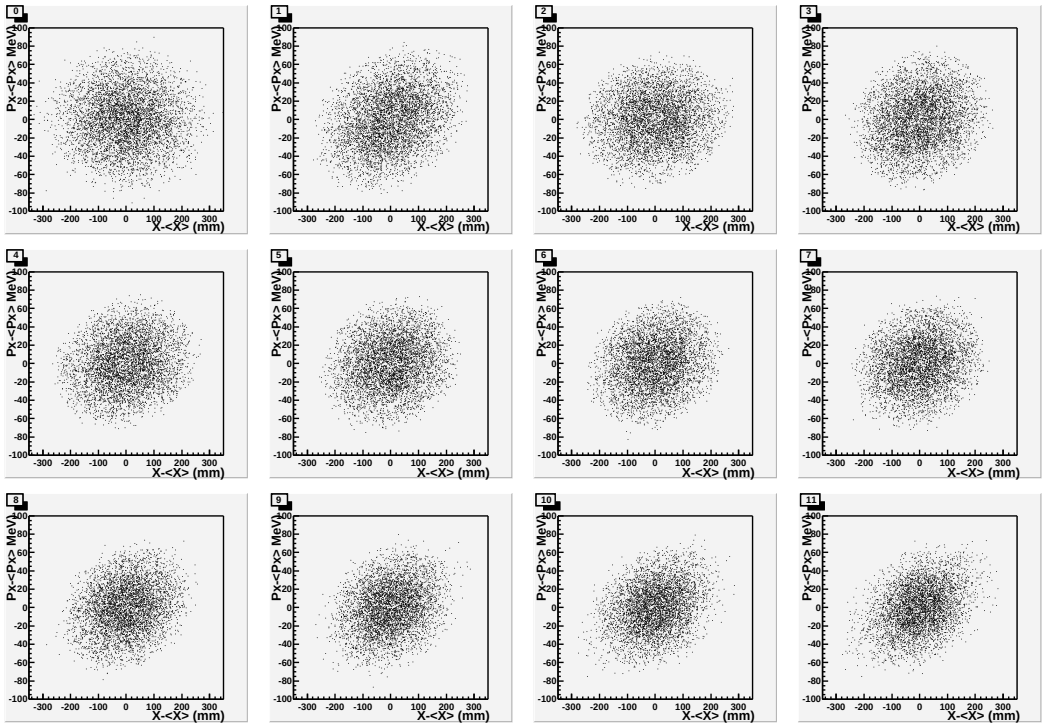

Figure 18: Evolution of the transverse phase space along the hard edge 44 MHz section. Each plot is a snapshot of the beam at the end of each cooling cell.

Fig. 15 shows the rapid increase of longitudinal emittance along the channel. The losses towards the end are related to running the the r.f. cavities on crest (longitudinal de-focusing). About 3% of the muons decay along the channel; if we ignored this effect as well as the acceptance losses at the beginning of the channel, transmission would increase to $\approx 96\%$. In Ref. [1], they probably did not run every cavity of the r.f. system at 90°. Fig. 16 also shows the angular momentum at the beginning of the channel and at the end of each of the 11 cooling cells.

Transverse cooling can be followed along the hard edge 44 MHz section in Figs 17, 18, which shows the evolution of the beam size and transverse momentum spread. A reduction in the physical size of the beam is apparent.

4.2 Pseudo-Realistic Results

The full cooling channel (the three sections) was implemented in GEANT4: geometry, solenoidal fields, acceleration, including r.f. tuning. The beam, however, was only followed through the first section with the objective of studying the transition from a hard-edge to a realistic design. A detailed simulation of the whole system awaits upcoming new developments in the channel design. Fig. 19 is based on a 5100 particles simulation which includes muon decay. It illustrates the performance of the 44 MHz section. As in the hard-edge version, σ_{p_x} remains basically constant along the channel, σ_x diminishes from 10.9 cm to 7.6 cm. Transverse emittance decreases from 25.1 mm to 13.3 mm, yielding a 0.53 cooling factor in each transverse direction. This factor is significantly lower than in the hard-edge version, due to the larger losses. The lower transmission, 55%, comes from larger losses in the beginning and towards the end of the section.

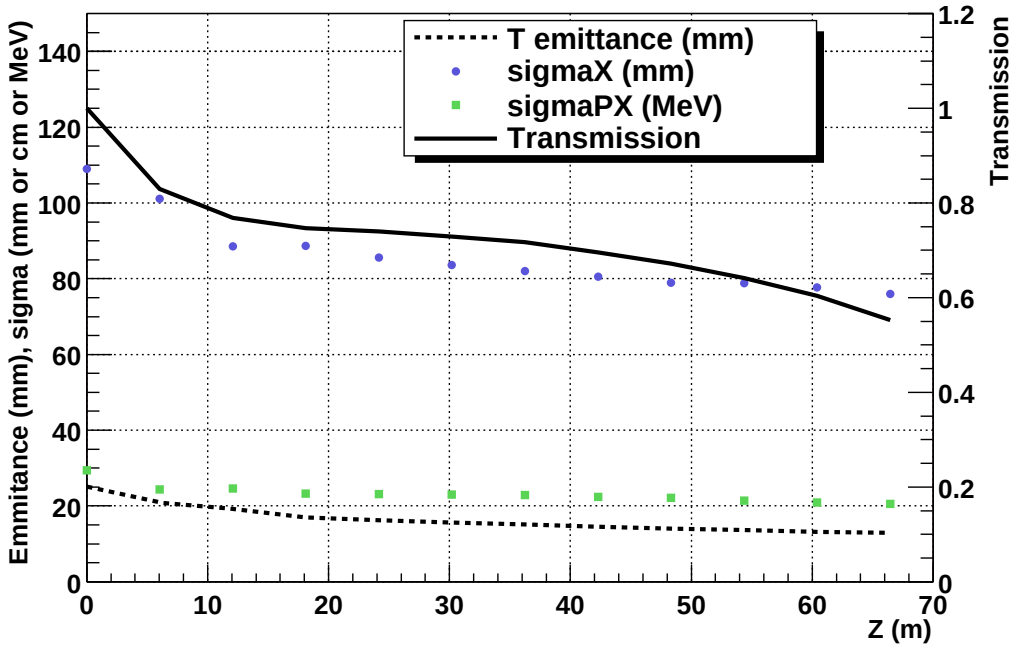

Figure 19: Performance of the pseudo-realistic version of the 44 MHz section of the cooling channel. Transverse emittance stands for ε_x.

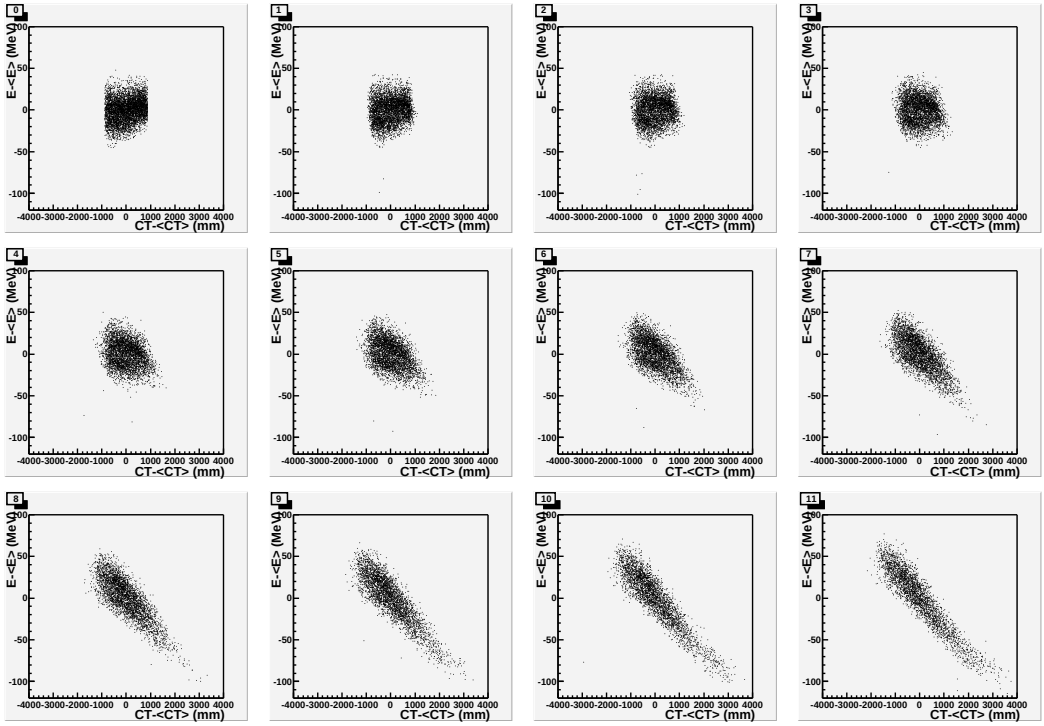

Figure 20: Evolution of longitudinal phase space along the pseudo-realistic 44 MHz section. Each plot is a snapshot of the beam at the end of each cooling cell.

Fig. 20 illustrates on the large losses in the last few cells. The longitudinal emittance grows faster when using the realistic r.f. system. The initial losses are large, mostly due to beam mismatch. The input beam is the output of a hard-edge design of the phase rotation system. The role of beam correlations and betatron resonances in this behavior will be discussed in the next section. Fig. 16 shows the angular momentum at the beginning of the channel and at the end of each of the 11 cooling cells. The cooling effect as a function of channel length can be observed in Figs 22, 23.

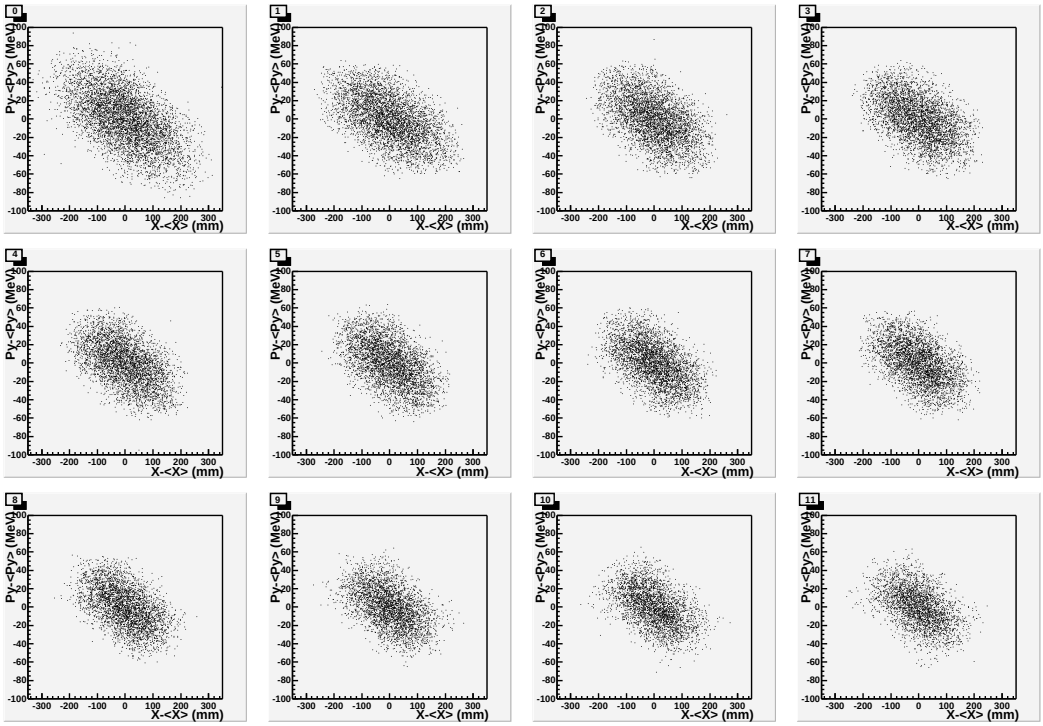

Figure 21: Evolution of the angular momentum along the pseudo-realistic 44 MHz section. Each plot is a snapshot of the beam at the end of each cooling cell.

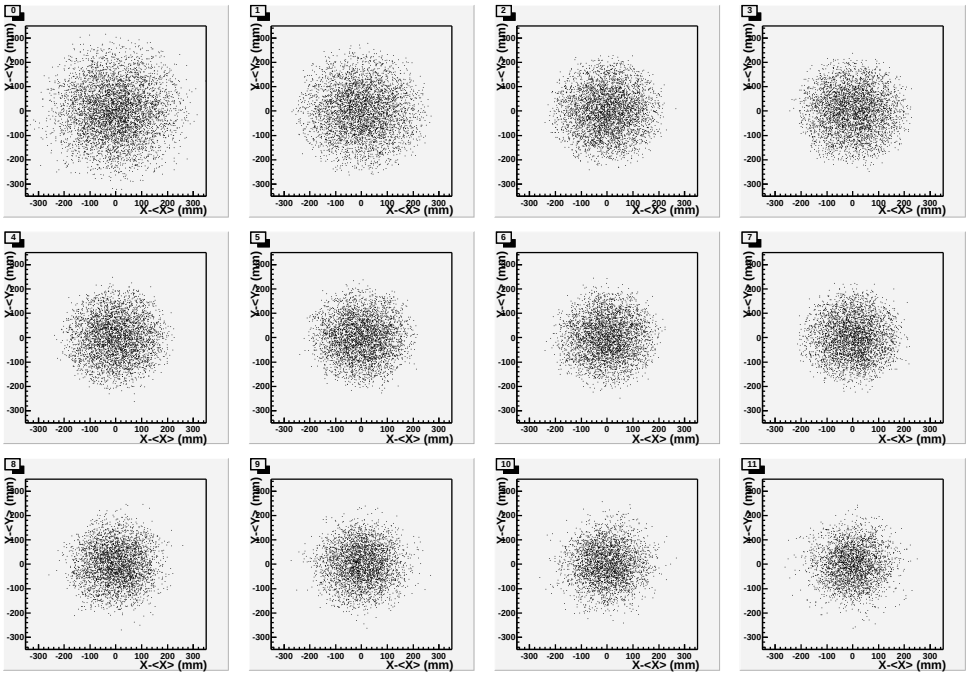

Figure 22: Evolution of the transverse physical size of the beam along the pseudo-realistic 44 MHz section. Each plot is a snapshot of the beam at the end of each cooling cell.

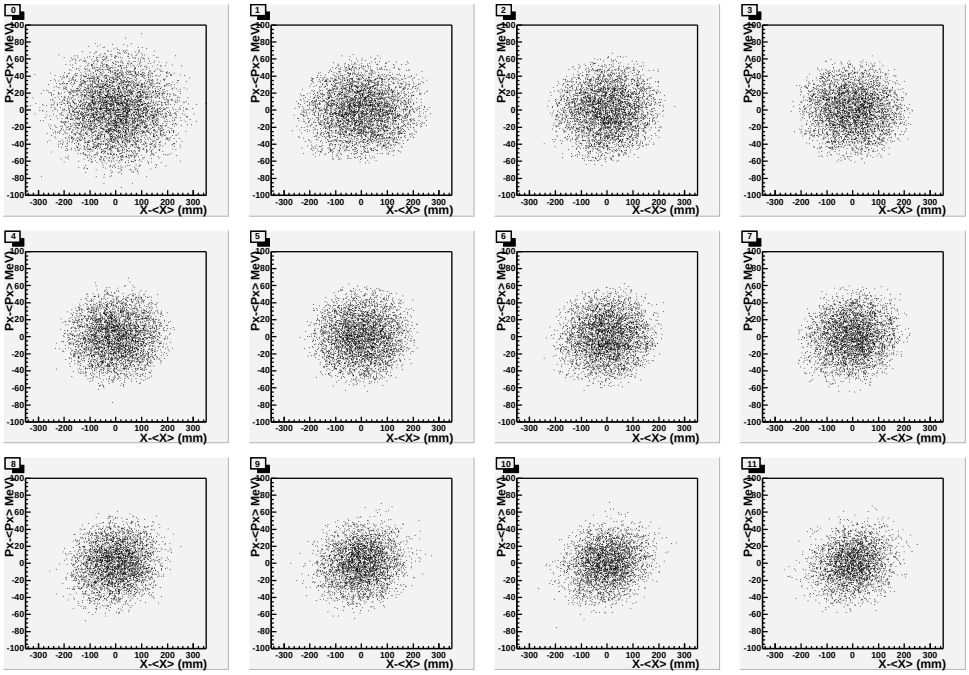

Figure 23: Evolution of the transverse phase space along the pseudo-realistic 44 MHz section. Each plot is a snapshot of the beam at the end of each cooling cell.

5 DESIGN STUDIES

In the previous section, we tested the simplistic assumption that performance would not be degraded as we went from a simple simulation to a more realistic one. We will now discuss how the

different channel and beam parameters determine the channel behavior.

5.1 Initial Correlations

A simple visual inspection of Figs. 3 and 9 tells us that a beam matched to the hard-edge 44 MHz section will not be matched to the realistic version proposed in this note. This accounts for most of the additional initial losses observed in Fig. 19 compared to Fig. 14. We modified the initial $p_y - x$ correlations following a simple recipe valid for a long solenoid:

$$p_x \rightarrow p_x - \frac{\alpha \times y \times B_\circ \times c}{2} \text{ and } p_y \rightarrow p_y + \frac{\alpha \times x \times B_\circ \times c}{2},$$

where, in our case, we took $B_\circ$ as the maximum amplitude of the oscillating B_z on axis. α is a free parameter to tune the correlations to obtain maximum transmission. The value α=1.4, corresponding to the beam shown in Fig. 24, gives the largest increment in transmission, from 55% to 69%. Fig. 24 also shows there is basically no change in the final transverse emittance of the beam.

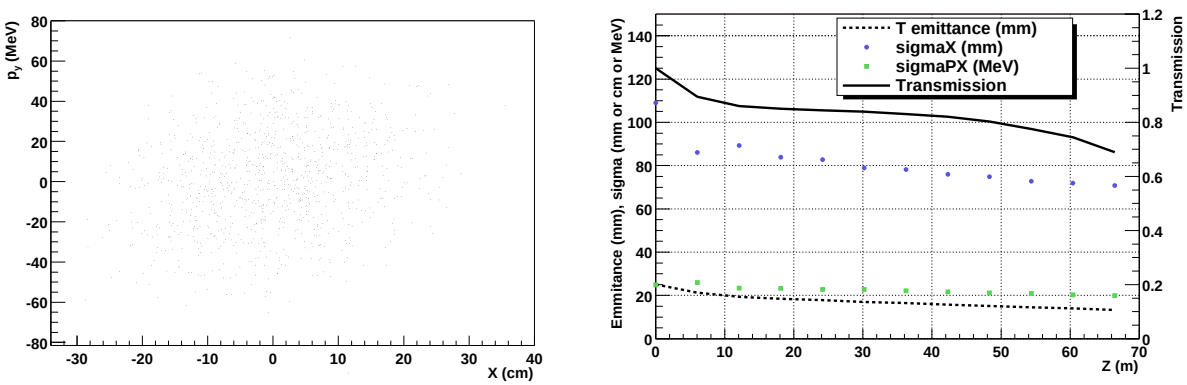

Figure 24: Left: initial $p_y - x$ distribution for the modified initial beam. Right: improved performance of the 44 MHz pseudo-realistic section using the modified beam. Transverse emittance stands for ε_x.

It should be possible to improve transmission further by injecting a beam with the right correlations, for example by running an arbitrary beam through an identical lattice but without acceleration or absorbers. The real question is whether such a beam could be produced and transmitted at the front-end (target, decay, phase rotation). If not, the losses would occur sooner or later when the beam entered the realistic 44 MHz lattice. The answer will come from a detailed simulation of the physics at the target, and appropriate matching sections to the realistic lattice.

5.2 Betatron Resonances

Equation 3 and Fig.1 in Ref. [8] allow us to compute the ranges of kinetic energy where the resonances of a periodic alternate solenoid system are located. While the 2π resonance is located at $E_{kin} = [9, 15]$ MeV, the π resonance is located at $E_{kin} = [29, 67]$ MeV. The system should be operated, though, above $E_{kin} \approx$ 90 GeV, far enough from the resonance boundary where the

β-function is strongly modulated. Since the average kinetic energy of the beam is 200 MeV with $\sigma_{E_{kin}}$=13.9, the average particle is more than 7σ away from the non-stable region, and resonances should not be an issue.

On the other hand, the magnetic field of the lattice we are using is more complex than a sinusoidal B_z on axis (see Fig. 3.2, Fig. 10). In order to study the resonances of our system, we used a Gaussian beam with parameters similar to those of the realistic beam (see Table 2). To avoid cooling or acceleration effects, we removed the r.f. system and the absorbers, keeping only the solenoids following the original pseudo-realistic geometry.

Table 2: Parameters of the Gaussian beam used to study resonances. The average kinetic energy is 200 MeV, $< x >=< y >=< p_x >=< p_y >= 0$.

σ_x	σ_{p_x}	σ_{cT}	σE
(cm)	**(MeV/c)**	**(cm)**	**(MeV)**
11	28	0	0

We then took a series of 200 particles runs, modifying the beam energy in steps of 3 MeV around the nominal E_{kin}=200 MeV. Figure 25 shows the transmission of the pseudo-realistic lattice as a function of the kinetic energy of the beam. A E_{kin} of 200 MeV is close to the optimal nominal energy for the channel. A resonance, however, seems to be closer to the operation energy than in the case of the ideal periodic alternate solenoid with sinusoidal $B_\circ$ field. One σ_E below E_{kin}=200 MeV, transmission drops by 7%; 2σ_E below nominal gives a 17% decrease, and 3σ_E below gives a 45% drop.

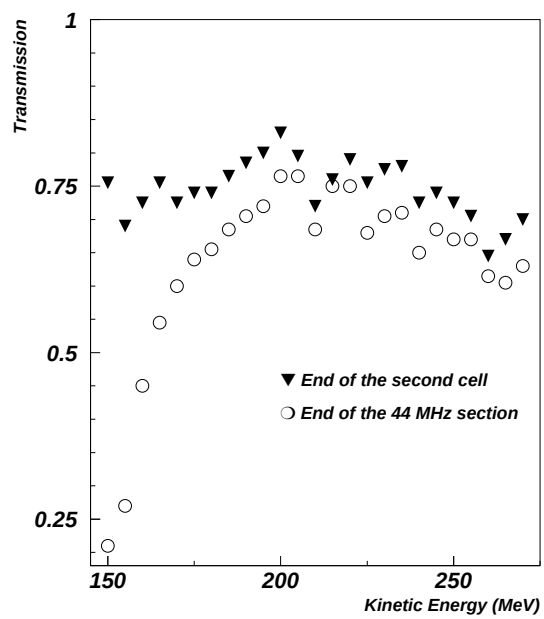

Figure 25: Transmission as a function of nominal beam energy for a Gaussian beam with fixed longitudinal parameters.

Using the information in Fig. 25, we divided the beam into two sets of particles: those with E_{kin} >200 MeV and those with E_{kin} <200 MeV. We verified that the transmission of the "positive" beam was higher than that of the "negative" beam by 4%. This confirms that although betatron resonances make a small contribution to particle losses in the pseudo-realistic 44 MHz section, the effect is not negligible.

5.3 *Geometry, Solenoids, and Cavities*

It is possible to modify the lattice to make the magnetic fields more well behaved. For example, Fig. 26 shows B_z on axis and $|B_r|$ at r=10.3 cm for a lattice where the extra space for the absorber has been removed. Now the system has one periodicity, the modulation to B_z has disappeared, and the amplitude of the $|B_r|$ peaks does not oscillate. In Fig. 27, the 52 cm gaps between solenoids have been reduced to 20 cm, in addition to removing the absorber space. The new system is very close to an ideal alternate solenoid channel, with B_z on axis well described by a sine function, and the double peaks have disappeared from $|B_r|$.

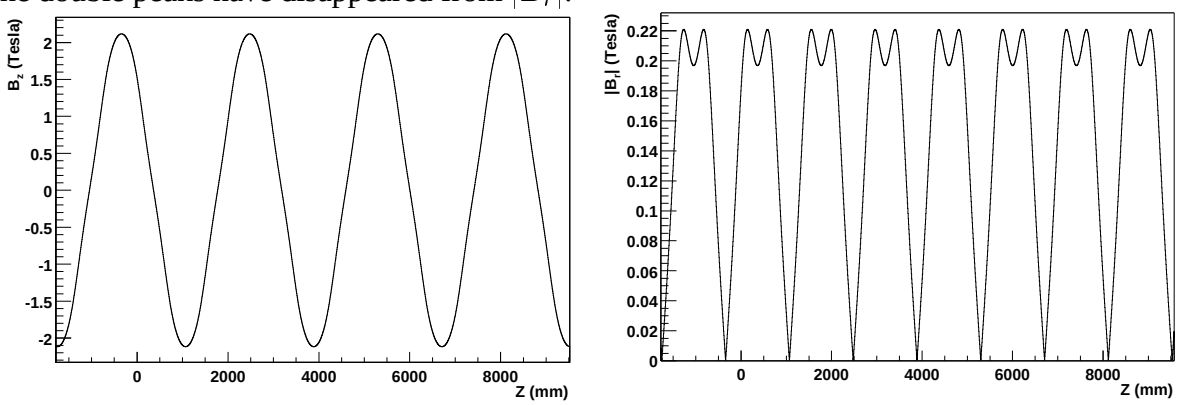

Figure 26: Left: $|B_r|$ versus z at r=10.3 cm for a modified 44 MHz lattice for which the absorber space has been removed. Right: $|B_r|$ versus z on axis for the modified lattice.

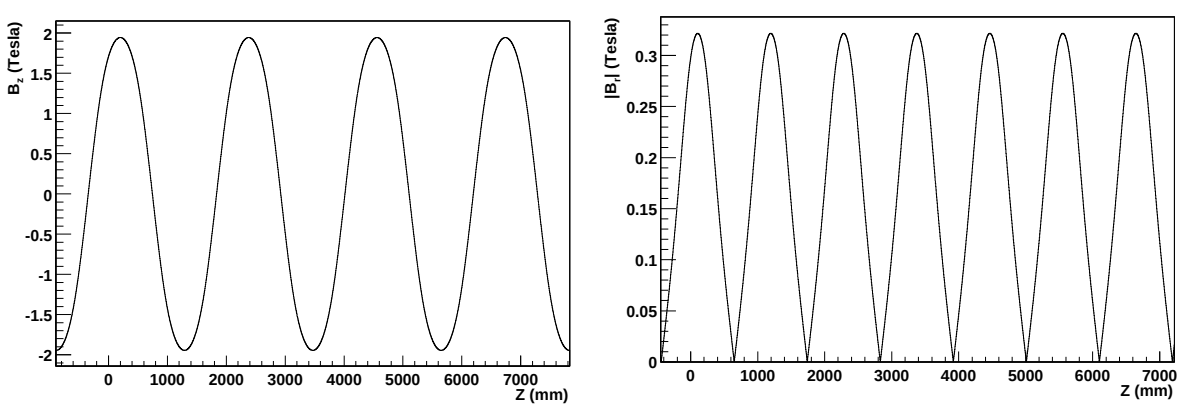

Figure 27: Left: $|B_r|$ versus z at r=10.3 cm for a modified 44 MHz lattice for which the absorber space has been removed. Right: $|B_r|$ versus z on axis for the modified lattice.

One way of reducing the 44 MHz lattice to the ideal sine case is to eliminate one of the four r.f. cavities and make the absorber shorter. That way we would have 1.4 m of free space to

place the absorber inside the magnet. There is the question on whether it is possible to reduce the relative space between magnets by re-designing the cavities or extending the lattice to include longer solenoids.

Another important issue is the polarity of the magnets. It is not necessary to invert the polarity at every magnet. Too many flip regions would add unnecessary engineering complexities. The polarity could be changed at every cell, but kept the same inside it.

A synchronous phase of 90° does not seem to be the optimum parameter to run the cavities. The r.f. system does not focus longitudinally that way, and therefore contributes to the longitudinal emittance growth and losses.

6 SUMMARY

In summary, we designed and coded a GEANT4 simulation of a pseudo-realistic version of the three sections of the 44/88 MHz cooling channel (CERN scheme). We verified that the GEANT4 and PATH simulations of the hard-edge version of the 44 MHz section gave consistent results: transmission $>85\%$ and a transverse cooling factor of ≈ 0.7 in each plane. We also studied the performance of the 44 MHz, and suggested modifications/improvements to the current design.

The code is flexible and allows changes in the lattice, r.f., absorber, and beam parameters, whenever the design is stable and ready for optimization. Modifications will be needed as the cooling channel is integrated to a more detailed design of the front-end and succeeding accelerator sections. There is an on-going effort[5] to replace the 44 MHz r.f. system in the first cooling section and make it 88 MHz all through the channel [5]. We therefore did not attempt to optimize the current lattice or beam parameters at this stage.

7 ACKNOWLEDGEMENTS

We thank Valeri Balbekov, Simone Gilardoni, Klaus Hanke, and Alessandra Lombardi, for useful discussions as well as information on the CERN channel design.

8 REFERENCES

[1] A. Lombardi, "A 40-80 MHz System for Phase Rotation and Cooling", CERN-NUFACT Note 34, August 2000.

[2] J. Gallardo (Editor), "A Feasibility Study-II of A Muon-Based Neutrino Source", June 2001. WWW.CAP.BNL.GOV/MUMU/STUDYII/FS2-REPORT.HTML

[3] Simulation package for accelerator studies developed at CERN.

[4] HTTP://WWWINFO.CERN.CH/ASD/GEANT4/GEANT4.HTML

[5] Alessandra Lombardi, private communication.

[6] R. Garoby, F. Gerigk, "Cavity Design for the CERN Muon Cooling Channel", CERN-NUFACT Note 87, 2001.

[7] Klaus Hanke, private communication.

[8] V. Balbekov, “New Design of Alternate Solenoid Cooling Channel for Neutrino Factory”, MuCool Note 98, March 2000.

[9] V. D. Elvira *et al.*, “Simulation of a Helical Channel Using GEANT4”, MuCool Note 193, February 2001.